Critical roles of the activation of ethylene pathway genes mediated by DNA demethylation in Arabidopsis hyperhydricity

Hongyang Gao[1], Xiuying Xia[1], and Lijia An[1]

[1]Dalian University of Technology

November 22, 2022

Abstract

Hyperhydricity often occurs in plant tissue culture, seriously influencing the commercial micropropagation and genetic improvement. DNA methylation has been studied for its function in plant development and stress responses. However, its potential role in hyperhydricity is unknown. In this study, we report the first comparative DNA methylome analysis of normal and hyperhydric Arabidopsis seedlings using whole-genome bisulfite sequencing. We found that the global methylation level decreased in hyperhydric seedlings, and most of the differentially methylated genes were CHH hypomethylated genes. Moreover, the bisulfite sequencing results showed that hyperhydric seedlings displayed CHH demethylation patterns in the promoter of the ACS1 and ETR1 genes, resulting in up-regulated expression of both genes and increased ethylene accumulation. Furthermore, hyperhydric seedling displayed reduced stomatal aperture accompanied by decreased water loss and increased phosphorylation of aquaporins accompanied by increased water uptake. While AgNO3 prevented hyperhydricity by maintained the degree of methylation in the promoter regions of ACS1 and ETR1 and down-regulated the transcription of both genes. AgNO3 also reduced the content of ethylene together with the phosphorylation of aquaporins and water uptake. Taken together, this study suggested that DNA demethylation is a key switch that activates ethylene pathway genes to enable ethylene synthesis and signal transduction, which may subsequently influence aquaporin phosphorylation and stomatal aperture, eventually cause hyperhydricity; thus, DNA demethylation plays a crucial role in hyperhydricity. These results provide insights into the epigenetic regulation mechanism of hyperhydricity, and confirm the role of ethylene and AgNO3 in hyperhydricity control.

Critical roles of the activation of ethylene pathway genes mediated by DNA demethylation in *Arabidopsis* hyperhydricity

Hongyang Gao[1,2], Xiuying Xia[1*], Lijia An[1]

1.School of Bioengineering, Dalian University of Technology, Dalian, Liaoning 116024, China

2. School of Traditonal Chinese Medicine, Guangdong Pharmaceutical University, Guangzhou 510006, China

Hongyang Gao, E-mail: ghy@gdpu.edu.cn

Lijia An, E-mail: bioeng@dlut.edu.cn

[*]**Corresponding author:** Xiuying Xia, E-mail: xx47@dlut.edu.cn, Tel:13504088133

Running Title: Role of DNA demethylation in hyperhydricity

Key words: hyperhydricity, DNA methylation, transcriptome, ethylene, aquaporin phosphorylation

Abstract

Hyperhydricity often occurs in plant tissue culture, seriously influencing the commercial micropropagation and genetic improvement. DNA methylation has been studied for its function in plant development and stress responses. However, its potential role in hyperhydricity is unknown. In this study, we report the first comparative DNA methylome analysis of normal and hyperhydric *Arabidopsis* seedlings using whole-genome bisulfite sequencing. We found that the global methylation level decreased in hyperhydric seedlings, and most of the differentially methylated genes were CHH hypomethylated genes. Moreover, the bisulfite sequencing results showed that hyperhydric seedlings displayed CHH demethylation patterns in the promoter of the *ACS1* and *ETR1* genes, resulting in up-regulated expression of both genes and increased ethylene accumulation. Furthermore, hyperhydric seedling displayed reduced stomatal aperture accompanied by decreased water loss and increased phosphorylation of aquaporins accompanied by increased water uptake. While $AgNO_3$ prevented hyperhydricity by maintained the degree of methylation in the promoter regions of *ACS1* and *ETR1* and down-regulated the transcription of both genes. $AgNO_3$ also reduced the content of ethylene together with the phosphorylation of aquaporins and water uptake. Taken together, this study suggested that DNA demethylation is a key switch that activates ethylene pathway genes to enable ethylene synthesis and signal transduction, which may subsequently influence aquaporin phosphorylation and stomatal aperture,

41 eventually cause hyperhydricity; thus, DNA demethylation plays a crucial role in
42 hyperhydricity. These results provide insights into the epigenetic regulation mechanism
43 of hyperhydricity, and confirm the role of ethylene and $AgNO_3$ in hyperhydricity control.
44
45
46
47
48

Introduction

DNA methylation, which refers to the addition of a methyl group to the fifth position of a cytosine in a DNA sequence, is one of the most widely investigated modes of epigenetic regulation (He et al. 2011). In plants, DNA methylation occurs in three different sequence contexts: CG, CHG and CHH (where H = A, C or T), and cytosine methylation levels (MLs) are controlled by various pathways, including *de novo* methylation, maintenance methylation, and demethylation pathways (Furner and Matzke 2011). DNA methylation is related to various genetic processes, including transcription regulation, transposable element (TE) silencing, imprinting, and genome stability (Cedar and Bergman 2012). The transcription of adjacent genes could also be influenced by the methylation of protein-coding genes and TE (Gazzani et al. 2003; Song et al. 2013). Several recent studies have revealed the crucial role of DNA methylation in the modulation of gene expression involved in plant developmental processes (Saze et al. 2003; Gehring and Henikoff 2009; Hsieh et al. 2009; Zemach et al. 2010; Chen and Zhou 2013) and in response to environmental stresses, such as high salinity, heat, drought, and cold (Mirouze and Paszkowski 2011; Sahu et al. 2013). Whole-genome bisulfite sequencing (WGBS) is a particularly powerful tool that can determine methylation patterns at single-nucleotide resolution (Cokus et al. 2008). WGBS has been widely adopted for DNA methylation analyses in plants such as maize (Li et al. 2014), apple (Xu et al. 2018), and oil palm (Ongabdullah et al. 2015).

As a common and powerful technique in agricultural industry practices and scientific research, tissue culture has been used for rapid propagation, virus-free seedling production and plant breeding improvements. However, the use of artificial medium and the exposure to extreme environments during *in vitro* culture may cause several physiological changes, among which the most universal is hyperhydricity (HH). Hyperhydric plantlets are morphologically and anatomically characterized by their translucent, thick and curled leaves; underdeveloped cuticles; malformations in stomatal morphology; accumulation of large starch grains within plastids; reduced numbers of chloroplasts per cell; and large intercellular spaces in the mesophyll (Dries et al. 2013; Gao et al. 2017a; Gao et al. 2017b). Hyperhydric cultures exhibit poor regeneration and survival abilities. Despite the availability of several approaches to ameliorate the negative effects of HH, such as adding ethylene biosynthesis inhibitors (Mensuali-Sodi et al. 1993), polyamines (Tabart et al. 2015), salicylic acid (SA) (Hassannejad et al. 2012) and K_2SiO_3 (Soundararajan et al. 2017) to the medium; optimizing the type and concentration of cytokinin (Ivanova and Staden 2011); using red and blue light-emitting diodes (Muneer et al. 2017); and enhancing the natural ventilation of culture vessels (Lai et al. 2005; Ivanova and Staden 2010), HH still leads to significant economic losses in agriculture, mainly because the molecular mechanism of HH is not yet clear.

Epigenetic alterations are more flexible than genetic variations. When environmental conditions change, epigenetic modifications allow species to more easily adapt to the new

environment (Xu et al. 2018). Many genome-scale methylome analyses have revealed that gene expression can be altered by changes in DNA methylation, which leads to visible phenotype under certain circumstances, especially when plants interact with different environmental factors to survive (Bräutigam et al. 2013; Sahu et al. 2013). HH is generally a result of the response of plants to stresses when explants are not placed in suitable *in vitro* environments, such as those with unusual growth regulator treatments, inefficient gas exchange, and high humidity. Various genetic, biochemical and physiological responses were involved in survival in response to abiotic stress (Hirayama and Shinozaki 2010). Previous studies have focused particularly on several physiological and biochemical responses of plantlets to HH. Changes in chlorophyll content, water content, antioxidant enzyme activity, reactive oxygen species (ROS) generation and plant hormones during HH have been reported (Saher et al. 2010; Tian et al. 2015; Sivanesan et al. 2016). Several transcriptomic and proteomic analyses have revealed changes that occur during HH and recovery from HH (Bakır et al. 2016; Muneer et al. 2016; Soundararajan et al. 2017). However, apparently, no studies have involved a global analysis of the extent and pattern of DNA methylation responses to HH. The potential roles of DNA methylation in HH development have barely been investigated.

An increasing amount of evidence has shown that excessive ethylene accumulation might be one of the key factors contributing to or promoting HH (Fal et al. 1999; Lai et al. 2005). Our previous studies (Gao et al. 2017b; Gao et al. 2017c) indicated that the

expression of ethylene signal transduction- and ethylene synthesis-associated genes increased in hyperhydric pink plantlets. Additionally, $AgNO_3$ could reduce the expression of ethylene signal transduction- and synthesis-associated genes, subsequently increasing water loss in hyperhydric plantlets and causing them to revert to a normal state. Despite these studies addressing some fundamental questions of the influences of ethylene on HH development, the possible role of DNA methylation in the regulation of gene expression during this process remains unknown.

Excessive water accumulation in plant tissue, especially in intercellular spaces, is the most characteristic symptom of HH. The overall water content increase is of great importance for the occurrence of HH (Dries et al. 2013). Although the mechanism of decreased water loss caused by stomatal closure mediated by excessive H_2O_2 accumulation in guard cells has been characterized by Gao et al. (Gao et al. 2017b), the water absorption mechanism has rarely been mentioned. Aquaporins play a key role in water uptake and transport. In our preliminary experiments, we found no alterations in the transcription level of aquaporin genes between hyperhydric and normal seedlings of both *Arabidopsis* and *Dianthus*. Qing et al. (Qing et al. 2016) recently proved that ethylene positively regulates water flux rates via activating aquaporin PIP2;1 phosphorylation in the leaves of *Arabidopsis* plants. However, the state of aquaporin phosphorylation in hyperhydric seedlings, as well as the function of aquaporins in water accumulation in hyperhydric tissue, is still unknown.

Here, we used RNA-seq and WGBS to explore the gene expression and cytosine methylation landscape of *Arabidopsis* hyperhydric seedlings on a genome-wide scale and to identify differentially methylated genes to reveal the epigenetic regulation mechanism of HH. The results showed that DNA methylation levels were significantly different between normal and hyperhydric seedlings. DNA demethylation of ethylene-related gene promoters may be a key switch that activates ethylene pathway genes to affect ethylene synthesis and signal transduction, which subsequently influence water metabolism, leading to HH. Together, these results advance our understanding of the function of DNA methylation and ethylene in HH development.

Results

Cultures with low concentrations of Gelrite induced HH in *Arabidopsis thaliana* seedlings

As shown in **Fig. 1**, seedlings maintained on medium solidified with 0.7% agar developed normally (**Fig. 1A**). However, seedlings cultured on medium solidified with 0.2% Gelrite exhibited a typical hyperhydric phenotype with elongated petioles and translucent, thick, and curled leaves (**Fig. 1A**), and the hyperhydricity rate reached 100%.

Comparison of global DNA methylation profiles between hyperhydric and normal *Arabidopsis* seedlings

To examine the overall methylation patterns of *Arabidopsis* responses to HH induced

148 by Gelrite, we performed WGBS on hyperhydric and normal seedlings, each with three
149 replicates. As many as ~37 million sequencing reads were generated per replicate. In
150 addition, up to ~80% and 75% of the total amount of cytosine was covered by more than
151 3 reads in the hyperhydric and normal seedlings, respectively (**Supplemental Table S1**),
152 indicating good library quality and high sequencing depth. We calculated Pearson
153 correlation coefficients for the three replicates of both samples; the coefficients were
154 0.995 and 0.992 for the hyperhydric and normal seedlings, respectively, indicating high
155 reproducibility of our bisulfite sequencing (BS-seq) results.

156 To obtain further insight into the differences in DNA methylation status between the
157 hyperhydric and normal seedlings, we analyzed the global ML of mC, mCG, mCHG and
158 mCHH in the hyperhydric and normal seedlings. The genome of the normal seedlings
159 comprised 11% (mC), 29% (mCG), 17% (mCHG) and 6% (mCHH) of the total
160 sequenced C, CG, CHG and CHH sites, respectively. Accordingly, the genome of the HH
161 seedlings comprised 10%, 28%, 17% and 5% of the C, CG, CHG and CHH sites,
162 respectively (**Supplemental Table S2**). The results showed that the MLs of mC, mCG
163 and mCHH in the hyperhydric seedlings were lower than those in the normal seedlings,
164 indicating that DNA demethylation may play an important role in HH development.

165 The distributions of mC in three sequence contexts revealed that methylcytosine was
166 most commonly found at CHH sites, and rarely occurred at CG and CHG sequences in
167 both the hyperhydric and normal seedling genomes. Nevertheless, compared with the

normal seedlings, the hyperhydric seedlings exhibited a decrease in the proportion of CHH methylation and a slight increase in the proportions of CHG and CG methylation (**Fig. 1B**).

We further evaluated the DNA methylation status of different genic regions. From a global perspective, the ML of CG in the upstream 2 kb and downstream 2 kb regions was much lower than that in the gene body regions; however, both the mCHH and mCHG types were abundant in the upstream 2 kb and downstream 2 kb regions but were detected at low levels in the gene bodies (**Supplemental Figure S1**). On the other hand, the ML of CG in different genic regions did not differ between the hyperhydric and normal seedlings. However, with respect to the CHG context, the DNA MLs in all three genic regions were significantly higher in the hyperhydric seedlings than in the normal ones. In the CHH context, the hyperhydric seedlings presented a dramatically higher ML than did the normal seedlings in the gene body region but a lower ML in the upstream 2 kb and downstream 2 kb regions (**Supplemental Figure S1**).

These results indicated that DNA methylation status and levels were significantly different between normal and hyperhydric seedlings. The decrease of CHH methylation ratio of the whole genome and the decrease of CHH methylation level of gene regulatory region may be related to HH occurrence.

Differentially methylated regions (DMRs) in the genomes of hyperhydric and normal seedlings

188 To investigate the methylation variation in *Arabidopsis* seedlings in response to HH,
189 we screened for DMRs between hyperhydric and normal seedlings. A total of 4066
190 significant DMRs, including 1016 hypermethylated and 3050 hypomethylated DMRs,
191 were identified. Hypomethylation was more common in the hyperhydric plants
192 (**Supplemental Figure S2**), and the number of DMRs was much greater in the CHH
193 context than in the CHG and CG contexts (**Fig. 1C**).

194 We further analyzed the distribution discrepancy of DMR in CHH context in different
195 gene regions. DMRs preferentially occurred in the promoter, repeat sequences regions,
196 and secondly in exon regions, while the transcription start site (TSS), untranslated region
197 (UTR) and transcription end site (TES) were less preferred (**Fig. 1C**). These data
198 indicated that DNA demethylation, particularly in the promoter and repeat sequences in
199 the CHH context, might be a key regulatory mechanism for HH occurrence.

200 The genes with DMRs within their body were considered DMR-associated genes
201 (DMGs), and those with DMRs within their promoter region (upstream 2 kb from the
202 TSS) were considered DMR-associated promoter genes (DMPs). We identified 1506
203 DMGs and 2980 DMPs in total. Notably, the number of DMGs and DMPs in the CHH
204 context was the highest among all three contexts (**Fig. 1D**).

205 We subsequently categorized these CHH DMGs and DMPs during HH development
206 by utilizing Gene Ontology (GO) analysis. The GO analysis revealed that DMGs
207 enrichment in biological processes largely related to cellular process (e.g.,

phenylpropanoid metabolic process) and response to stimuli (e.g., response to stress, response to chemicals, response to abiotic stimulus and response to hormones) **(Supplemental Figure S3)**. CHH DMPs were mostly enriched in cellular catabolic processes and proteolysis pathway **(Supplemental Figure S3)**.

These results suggest that the changes in methylation of genes involved in stimuli response may participate in the occurrence and development of HH .

Differentially expressed genes (DEGs) in hyperhydric and normal seedlings

To explore the potential transcriptional consequences of widespread methylation changes related to HH, we performed RNA-seq on the same normal and hyperhydric seedlings that were used for WGBS. A total of 2197 transcripts, including 1212 upregulated and 985 downregulated transcripts, were differentially expressed in the hyperhydric seedlings compared with the normal seedlings (**Supplemental Fig. S4**).

The detailed assignments of the DEGs and pathways as determined by MapMan are shown in **Fig. 2A**. We noticed that an abundance of DEGs were enriched in the ‘abiotic stress’ ‘signaling’ and ‘cell wall’ pathways. Numerous genes involved in hormone signaling pathways, including those of auxin, ethylene and jasmonic acid (JA), were found to be differentially expressed in hyperhydric seedlings compared with normal seedlings. Some genes encoding transcription factors (TFs) such as ethylene response factor (ERF), MYB and WRKY were also differentially expressed. Furthermore, a large

number of genes associated with redox equilibrium were significantly enriched in the hyperhydric seedlings. The above results indicated that the expression modulation of genes involved in various pathways, such as those involving abiotic stress, hormone signaling, and redox, might be correlated with physiological changes in hyperhydric seedlings.

Correlation analysis between genes with DMRs and DEGs

To explore the influence of DNA methylation on the expression of neighbouring genes, we assessed the relationship between genes with DMRs and transcript abundance on a genome-wide scale. Approximately 6.9% (153) of the DEGs were associated with DMGs; among these DEGs, 25 (16.3%) were hypermethylated with downregulated expression levels in hyperhydric seedlings compared with normal seedlings, and 64 (41.8%) were hypomethylated with upregulated expression levels. However, 27 (17.6%) upregulated and 38 (24.8%) downregulated genes were hypermethylated and hypomethylated, respectively (**Fig. 2B**). On the other hand, a total of 183 DEGs were associated with DMPs; among these DEGs, 14 (7.6%) were hypermethylated with downregulated expression levels in the hyperhydric seedlings compared with the normal seedlings, and 82 (44.8%) were hypomethylated with upregulated expression levels. Furthermore, 70 (38.2%) downregulated and 19 (10.4%) upregulated genes were hypomethylated and hypermethylated, respectively (**Fig. 2C**).

The correlation between gene transcription level and DNA methylation status in

different contexts was further analyzed. Significant negative correlations were revealed between gene expression level and CG hypo-ML in both the gene body (rho = –0.61, P = 0) and promoter (rho = –0.43, P = 0) regions (**Supplemental Fig. S5A**). The expression of DMR-associated DEGs was not significantly correlated with methylation status in the CHG context (P > 0.05) (**Supplemental Fig. S5B**). Gene expression changes were predominantly negatively correlated with CHH MLs in both the gene body and promoter regions, and hypomethylation tended to upregulate gene expression, while hypermethylation tended to downregulate gene expression (**Supplemental Fig. S5C**).

The above results indicated that the expression of most DMR-associated DEGs was negatively correlated with methylation levels. In general, the expression of genes associated to hypermethylated DMRs was downregulated, while the expression of genes associated to hypomethylated DMRs was upregulated. Some of the DMR-associated DEGs were positively correlated with methylation levels. Furthermore, compared with those in the other contexts, changes in methylation in the CHH context are more important in the regulation of DEG expression.

Ethylene plays a crucial role in *Arabidopsis* HH development

Excess ethylene accumulation is confirmed to be associated with HH in some studies (Kevers et al. 2004; Gao et al. 2017b). Our transcriptome and methylome analyses indicated that many genes involved in the ethylene synthesis and signaling pathway were identified as DMR-associated DEGs (**Supplemental Fig. S6** and **Table S3**). We further

explored the detailed function and the underlying mechanism of ethylene in the occurrence and development of HH.

We noticed that ethylene-insensitive mutants (*ein2-5, etr1-9, etr1-3*) cultured on HH induction medium containing low concentration of Gelrite (0.2%) did not develop HH, while ABA-insensitive mutants (*abi5-1*, *abi4-101*, *abi2-1*) did exhibit HH symptoms (**Supplemental Fig. S7**). We further explored the function of $AgNO_3$ on HH by adding $AgNO_3$ to the above HH induction medium. Most seedlings developed no symptoms of HH after 14 days of culture in medium supplemented with $AgNO_3$, attaining normal development as shown in **Fig. 3A**. Moreover, compared with that of seedlings grown on medium without $AgNO_3$, the endogenous water content and ethylene level in the seedlings grown on $AgNO_3$-supplemented medium decreased (**Fig. 3B and C**). These results indicated that ethylene plays a vital role in the occurrence and development of HH in *Arabidopsis* and that $AgNO_3$ can prevent HH and reduce the ethylene content.

The DNA ML of the *ACS1* and *ETR1* promoters decreased in hyperhydric seedlings, and the expression of ethylene signaling pathway genes increased

Based on the methylome and transcriptome analysis results, we selected the *ACS1* and *ETR1* genes, which are involved in the ethylene pathway, to analyse the differences of the methylation pattern in promoter and the transcript abundance between hyperhydric and normal seedlings. The DMRs existed in the promoter sequences of these two genes were subjected to bisulfite sequencing to detect methylation, and qPCR was performed to

examine mRNA levels. Seedlings cultured in agar (‘Normal’), 0.2% Gelrite (‘HH’) and Gelrite supplemented with $AgNO_3$ (‘HH +$AgNO_3$’) media were used as materials. As shown in **Fig. 3D**, the *ACS1* and *ETR1* genes displayed hypomethylation patterns and increased transcription in ‘HH’ materials compared with ‘Normal’ materials. Nevertheless, these two genes displayed a hypermethylation pattern and exhibited decreased transcription in the ‘HH+$AgNO_3$’ materials compared with the ‘HH’ materials.

We further measured the dynamic changes in expression levels of the ethylene biosynthesis-associated genes *SAM*, *ACS1* and *ACO*; the ethylene receptor genes *ETR1* and *ETR2*; and the ethylene-responsive factor genes *ERF12* and *ERF113*. Our real-time qPCR results showed that the expression levels of ethylene pathway genes were increased in the ‘HH’ materials compared with the ‘Normal’ materials. However, decreased numbers of transcripts of ethylene-related genes and reduced ethylene content were detected in the ‘HH+$AgNO_3$’ materials (**Supplemental Figure S8**). The above results suggested that promoter hypomethylation of *ACS1* and *ETR1* may upregulate gene expression and active the ethylene signaling pathway and trigger HH and that $AgNO_3$ may suppress the ethylene signaling pathway and prevent HH development by hypermethylating the promoter and downregulating the expression of ethylene-related genes.

Phosphorylation of aquaporin PIP2;1 and water uptake rates increased in hyperhydric seedlings

307 The PIP2;1 protein from three types of seedlings was investigated via
308 immunoblotting analysis (**Fig. 4A**). The results demonstrated that phosphorylation of
309 PIP2;1 was significantly increased in the ‘HH’ materials. However, the phosphorylation
310 levels of PIP2;1 in the ‘HH+$AgNO_3$’ materials were lower than those in the ‘HH’
311 materials and were similar to those in the ‘Normal’ materials after 14 days of culture.

312 Phosphorylation of plant aquaporin proteins directly affects water channel activity.
313 Ethylene can enhance the phosphorylation of PIP2;1, increasing the water permeability of
314 leaf protoplasts (Qing et al. 2016). Here, we used swelling assays to investigate the water
315 permeability of different types of samples. Significant differences in relative volume
316 (*V/Vi*) were detected among protoplasts from different samples. The protoplasts generated
317 from the ‘HH’ materials exhibited faster swelling rates than did the ‘Normal’ materials
318 after 14 days of culture. However, the swelling rate of the ‘HH+$AgNO_3$’ materials was
319 slower than that of the ‘HH’ materials (**Fig. 4B**).

320 We also measured the osmotic water permeability coefficient (*Pos*) of the protoplasts
321 to analyse their water uptake capacity in different seedlings. Our results showed that the
322 *Pos* was higher in the ‘HH’ materials than in the other seedlings, but compared with that
323 of the ‘HH’ materials, the *Pos* of the ‘HH+$AgNO_3$’ materials decreased after 14 days of
324 culture (**Fig. 4C**). The incremental levels of osmotic water permeability were highly
325 consistent with the altered phosphorylation levels measured by immunoblotting analysis.
326 These results implied that ethylene may positively affects the phosphorylation of PIP2;1

and the water uptake capacity in hyperhydric seedlings.

Stomatal aperture and water loss decreased in hyperhydric seedlings

The H_2O_2 levels in the guard cells of 'HH' materials were markedly higher than those of 'Normal' materials, while the H_2O_2 levels in the 'HH+$AgNO_3$' materials were significantly lower than those in the 'HH' materials **(Fig. 5A)**. Accompanied by an increase in the H_2O_2 levels in guard cells, both the water loss rate and stomatal aperture of the 'HH' materials significantly decreased. However, compared with the 'HH' materials, the 'HH+$AgNO_3$' materials exhibited an increase in the water loss rate and stomatal aperture (**Fig. 5B-D**). These results suggest that the decrease in the water loss rate and stomatal aperture in hyperhydric *Arabidopsis* seedlings might be mediated by the production of H_2O_2 in guard cells as a result of induction by excessive amounts of ethylene.

Discussion

HH is a consequence of plant responses to wounding or environmental stresses when transferring excised explants to unsuitable conditions (Kevers et al. 2004; Ivanova and Staden 2011). It has been shown that HH induces morphological and physiological changes in whole plantlets and results in significant economic losses in the commercial micropropagation industry (Gao et al. 2017a). DNA methylation is one of the main epigenetic mechanisms in higher eukaryotes and plays an important role in both

346 regulating plant growth and development and responding to abiotic stress (Gazzani et al.
347 2003; Hsieh et al. 2009; Mirouze and Paszkowski 2011; Xu et al. 2018). Nevertheless,
348 the methylation regulatory mechanism of HH is still unknown. It is worth elucidating this
349 issue to determine the epigenetic regulatory network of the occurrence and development
350 of HH.

351 In the present study, we first analyzed the DNA methylation profiles of hyperhydric
352 and normal seedlings using a WGBS approach. Compared with the normal seedlings, the
353 hyperhydric seedlings showed decreased proportion of CHH methylation and reduced
354 MLs percentage of CHH sites (**Fig. 1B and Supplemental Table S2**). We profiled the
355 DNA methylome of the hyperhydric and normal seedlings, which revealed numerous
356 HH-associated DMRs. Notably, the DMRs in the CHH context were more frequent than
357 those in the CG and CHG contexts, and most of the DMRs were hypomethylated and
358 occurred in regulatory regions, such as promoter and repeat regions (**Fig. 1C**).
359 Furthermore, the combined analysis of the transcriptome and methylome revealed that the
360 expression of most DMR-associated DEGs is negatively correlated with changes in
361 methylation and that the changes in methylation, especially hypomethylation, in the CHH
362 context are more important in the regulation of DEG expression (**Supplemental Figure**
363 **S5**). These results suggest that CHH demethylation in gene regulatory regions may be
364 predominantly responsible for activating the transcription of surrounding genes, such as
365 functional regulators or signal response factors, that are involved in metabolism and

366 stress resistance; thus, CHH demethylation may play unique roles in the development of
367 HH morphological characteristics and physiological response processes.

368 However, many DEGs were not regulated by methylation status of promoter or gene
369 body (**Fig. 2B and C**). This phenomenon might be a result of methylation-dependent
370 alterations to transcription networks, such as methylation of TFs, TEs and methylation of
371 genes involved in hormone signaling pathways. Changes in TFs can further affect the
372 expression levels of target genes together with abundant downstream genes. Changes in
373 hormone signaling, such as that of SA, ethylene and JA, could mediate stress responses
374 as well as numerous developmental processes. Our results showed that many CHH
375 DMR-associated genes were involved in responses to hormone signals (**Supplemental**
376 **Figure S3**). We observed that, in hyperhydric plants, many TF genes including members
377 of the MYB and ERF classes, exhibited methylation changes (**Supplemental Table S3**).
378 Consistent with this result, a global transcriptional analysis of the hyperhydric and
379 normal seedlings revealed that numerous hormone signaling genes and TFs were
380 differentially expressed (**Fig. 2A**). In addition, many repeats and TEs were also
381 demethylated in the hyperhydric seedlings (**Fig. 1C and Supplemental Figure S2**).
382 These results implied that DNA demethylation might also alter the transcription of TFs,
383 TEs or genes involved in hormone pathways and further regulate biological processes
384 that respond to environmental influences, consequently leading to the development of HH
385 symptoms. However, further functional analysis is necessary.The role of ethylene in HH

386 is still debated. It has been reported that high concentrations of ethylene accumulate in
387 hyperhydric culture in certain plant species (Franck et al. 2004; Gao et al. 2017b). Some
388 researchers have shown that excess ethylene accumulation is one of the key factors that
389 causes HH (Lentini et al. 1988; Kevers et al. 2004). It has also been reported that
390 ethylene has no effect on the development of HH in *Arabidopsis* seedlings cultured on
391 Gelrite (Dries et al. 2013). In our present study, ethylene-insensitive mutants (*ein2-5*,
392 *etr1-9*, and *etr1-3*) cultured on Gelrite did not exhibit HH symptoms, which is in contrast
393 with the results of Dries (Dries et al. 2013), while ABA-insensitive mutants (*abi5-1*,
394 *abi4-101*, and *abi2-1*) displayed HH symptoms (**Supplemental Fig. S7**). Moreover, the
395 seedlings cultured in $AgNO_3$-supplemented media did not exhibit HH symptoms (**Fig.**
396 **3A**). These results verify that ethylene plays a vital role in the development of HH caused
397 by Gelrite in *Arabidopsis*.

398 To examine the regulatory function of methylation in ethylene signaling during HH
399 development, we analyzed the DNA methylation patterns of the promoters of the *ACS1*
400 and *ETR1* genes in three types of seedlings that were separately cultured in agar (Normal),
401 Gelrite (HH) and Gelrite supplemented with $AgNO_3$ media. Bisulfite sequencing analysis
402 revealed that, compared with those of the normal seedlings, the promoters of the *ACS1*
403 and *ETR1* genes of the hyperhydric seedlings displayed demethylated patterns and
404 upregulated transcription (**Fig. 3**). Nevertheless, $AgNO_3$ maintained the degree of
405 methylation in the promoter regions of *ACS1* and *ETR1* and downregulated the

406 transcription of both genes. These results suggested that DNA methylation and
407 demethylation might regulate ethylene signaling by acting as a control switch for *ACS1*
408 and *ETR1* expression and that $AgNO_3$ can disrupt the ethylene signaling pathway by
409 maintaining methylation of the *ACS1* and *ETR1* promoters.

410 Qing et al. (Qing et al. 2016) showed that ethylene positively regulates the water flux
411 rate via the phosphorylation of the aquaporin PIP2;1 in the leaves of *Arabidopsis*. In the
412 present study, the ethylene content in the normal seedlings was significantly lower than
413 that in the hyperhydric seedlings. We hypothesize that ethylene-regulated
414 phosphorylation of aquaporins might contribute to water accumulation in hyperhydric
415 tissue. Consistent with our assumption, the phosphorylation of PIP2;1 significantly
416 increased in the hyperhydric seedlings, which led to increased water uptake in those
417 seedlings. Nevertheless, $AgNO_3$ reduced the content of ethylene together with the
418 phosphorylation of the PIP2;1 isoform and water uptake (**Fig. 4**).

419 Taken together, we propose that the development of HH might occur via a
420 mechanism that involves the regulation of DNA methylation and the expression of genes
421 associated with the ethylene signaling pathway. As shown in **Fig. 6**, the unsuitable culture
422 environment (such as low concentration Gelrite) and the process of separating the
423 explants represents a considerable stress to plants and evokes stress responses within cells;
424 these responses could potentially lead to the demethylation of genes involved in the
425 ethylene pathway. Ethylene synthesis and signal transduction would subsequently

increase, which might induce both phosphorylation of aquaporins and stomatal closure, after which water loss would decrease and water uptake would increase. As a result, excessive amounts of water accumulate in the tissues, and HH symptoms occur. $AgNO_3$ prevents HH might by blocking the ethylene pathway by maintaining the ML of ethylene signaling pathway genes through a certain mechanism. The establishment of the possible mechanisms on HH occurrence and HH reversal is important in future efforts to reduce hyperhydricity in the tissue culture industry. Nevertheless, the specific functions of most related genes, such as ethylene pathway genes, aquaporin genes as well as other DMGs and DMPs, in the development and reversion of hyperhydricity remain unclear. Whether manipulation of some important genes will change the level of hyperhydricity remains to be studied.

Experimental procedures

Plant growth and treatments

Arabidopsis thaliana (Col-0) seeds were sterilized with 75% (v/v) ethanol for 1 min, after which they were subsequently sterilized three times for 1 min with 100% (v/v) ethanol. The sterilized seeds were transferred to Petri dishes that contained Murashige and Skoog (MS) media supplemented with 1.5% (w/v) sucrose and solidified with 0.7% (w/v) micro-agar (Sangon Biotech, Shanghai, China) or 0.2% (w/v) Gelrite (Sigma, St Louis, MO, USA). The seeds were then cultured in the dark for 3 days at 4 °C and then

transferred to a growth chamber under a 16 h light (30 μmol m^{-2} s^{-1})/8 h dark photoperiod at 21 °C.

Four-day-old seedlings cultured on micro-agar were transferred to fresh MS media supplemented with 0.7% (w/v) micro-agar; these seedlings were considered normal ones. To induce HH, 4-day-old seedlings cultured on Gelrite were transferred to Petri dishes (nine seedlings per dish) that contained MS media solidified with 0.2% (w/v) Gelrite. To prevent the occurrence of HH, 4-day-old seedlings cultured on Gelrite were transferred to MS media that was solidified with 0.2% (w/v) Gelrite and supplemented with 29.4 μmol L^{-1} $AgNO_3$.

At 10 days after being transferred, the seedlings were removed from the Petri dishes, frozen in liquid nitrogen and stored at −80 °C until further use. Three biological replicates were used for the experimental setup.

Seeds of wild type, *ein2-5*, *etr1-9*, *etr1-3*, *abi5-1*, *abi4-101* and *abi2-1* were obtained from the Nottingham *Arabidopsis* Stock Centre (Nottingham, UK; http://www.arabidopsis.info/).

RNA extraction and transcriptome sequencing

A total amount of 3 μg of RNA per sample was used as input material for RNA sample preparations. Sequencing libraries were generated using a NEBNext® Ultra™ RNA Library Prep Kit for Illumina® (NEB, USA) in accordance with the manufacturer's

464 recommendations. To select cDNA fragments that were preferentially 150~200 bp in
465 length, the library fragments were purified with an AMPure XP system (Beckman Coulter,
466 Beverly, USA). Clustering of the index-coded samples was performed on a cBot Cluster
467 Generation System using a TruSeq PE Cluster Kit v3-cBot-HS (Illumina) according to
468 the manufacturer's instructions. After filtering and removing the adapters and low-quality
469 reads, the clean reads were aligned to the *Arabidopsis* reference genome by TopHat
470 v2.0.12. HTSeq v0.6.1 was then used to count the read numbers mapped to each gene,
471 after which the fragments per kilobase of transcript sequence per millions base pairs
472 sequenced (FPKM) of each gene was calculated according to its length and read count.
473 The DESeq R package (v1.18.0) was used for differential gene expression analysis. The
474 resulting *P*-values were adjusted by Benjamini and Hochberg's approach for controlling
475 the false discovery rate. Genes with an adjusted *P*-value < 0.05 were considered
476 differentially expressed.

477 **DNA extraction and BS-seq library construction**

478 The genomic DNA isolated from normal and hyperhydric seedlings was processed for
479 bisulfite sequencing. DNA extraction and BS-seq library construction were conducted as
480 previously described (Xu et al. 2018), with three biological replicates per sample.
481 Bismark software (v0.16.3) (Krueger and Andrews 2011) was used to align the sequences
482 of the bisulfite-treated reads to a reference genome, according to the method described
483 previously (Jin et al. 2018). Read pairs that shared the same coordinates in genome were

484 considered duplicates and were removed before methylation state calling, thus avoiding
485 potential ML calculation bias. The results of the methylation extraction were transformed
486 to bigWig format for visualization using IGV browse.

487 To calculate the ML of the sequences, we divided the sequence into multiple bins that
488 were 10 kb in size. The sum of the methylated and unmethylated read counts in each
489 window was calculated. The ML for each window or C site shows the fraction of
490 methylated Cs and is defined as:

491 $$\mathrm{ML(C)} = \frac{reads(\mathrm{mC})}{reads(\mathrm{mC}) + reads(\mathrm{C})}$$

492 In the end, the ML was further corrected with the bisulfite non-conversion rate. Given
493 the bisulfite non-conversion rate ‘r’, the corrected ML was estimated as:

494 $$ML_{(corrected\ )} = \frac{ML - r}{1 - r}$$

495 The percentage of methylation was defined as the proportion of mCs on the total C
496 sites. The relative proportion of mCs in the three contexts was defined as the proportion
497 of mCG, mCHG and mCHH on the total mC sites (Xu et al. 2018).

498 **Analysis of DMRs**

499 The DMRs were identified using DSS software (Feng et al. 2014; Wu et al. 2015;
500 Park and Wu 2016), and the core of DSS is a new dispersion shrinkage method for
501 estimating the dispersion parameter from gamma-Poisson or beta-binomial distributions.

On the basis of the distribution of DMRs throughout the genome, we defined the genes related to DMRs as those whose gene body region (from the TSS to the TES) or promoter region (upstream 2 kb from the TSS) overlapped with the DMRs. A GO enrichment analysis of genes related to DMRs was implemented with the GOseq R package (Young et al. 2010); during this analysis, the gene length bias was corrected. GO terms with corrected P-values less than 0.05 were considered significantly enriched by DMR-related genes.

Bisulfite sequencing

One microgram of DNA was treated with sodium bisulfite using an EZ DNA Methylation-Gold Kit (Zymo Research, Orange, CA) in accordance with the manufacturer's instructions. The DNA was amplified by PCR with ExTaq (TaKaRa, Dalian, China). The sequences of *ACS1* (chromosome 3 sequence 22766812-22767126) and *ETR1* (chromosome 1 sequence 24732763-24733122) were analyzed. The sequences of primers used are shown in **Supplemental Table S4**. The PCR products were cloned into a pMD18-T simple vector (TaKaRa, Dalian, China), and the clones were sequenced.

Quantitative real-time PCR (qRT-PCR)

RNA was isolated with an RNeasy Plant Mini Kit (Sangon Biotech, China), and cDNA synthesis was performed with a PrimeScript^{TM} RT reagent kit in conjunction with gDNA Eraser (TaKaRa, Dalian, China). qRT-PCR analysis was performed with a

521 Rotor-Gene 3000 PCR instrument (Corbett Research, Australia) using a SYBR Premix
522 Ex Taq^{TM} Kit (TaKaRa, Dalian, China). The experiments were performed at least three
523 times under identical conditions, and *actin* served as an internal control. The primers used
524 are listed in **Supplemental Table S5**.

525 **Measurements of the relative water content, ethylene content, water loss rate,**
526 **stomatal aperture and H_2O_2 levels in guard cells**

527 Seedlings were collected to measure their endogenous ethylene content by the ELISA
528 method with an ethylene ELISA kit (Tsz Biosciences, USA) according to the
529 manufacturer's instructions. The rate of water loss (WLR), relative water content,
530 stomatal aperture and H_2O_2 levels in guard cells were measured in accordance with our
531 previous studies (Gao et al. 2017b).

532 **Antibody preparation and immunoblot assays**

533 The anti-PIP2;1 rabbit polyclonal antibodies and anti-*p*S283 polyclonal antibodies
534 used in this study were made commercially (Sangon Biotech, Shanghai, China). The
535 proteins were extracted from *Arabidopsis* tissue with a One Step Plant Active Protein
536 Extraction Kit (Sangon Biotech, Shanghai, China) and used for the immunoblot analyses,
537 fractionated on a 10% SDS-PAGE gel and immobilized onto a polyvinylidene fluoride
538 membrane (Sangon Biotech, Shanghai, China), which was probed with
539 anti-PIP2;1-specific polyclonal antibodies (anti-PIP2;1) and anti-*p*S283 polyclonal

antibodies.

Protoplast swelling assays

Leaf protoplasts from seedlings were prepared in accordance with the methods of Wu et al. (Wu et al. 2013). Before the experiment, the protoplasts were stored for 15 min at room temperature. The protoplast swelling assay method was performed according to previously described methods (Qing et al. 2016).

Pos values of the protoplast membrane calculations

In accordance with previous results (Qing et al. 2016), the osmotic permeability function was expressed as:

$$\ln\frac{a-\beta+a\beta-V_r}{(1-\beta)(a-1)}+\frac{V_r-1}{a(1-\beta)}=-\frac{P_{OS}v_wAC_f}{aV_i}t$$

where V_r is the relative volume of a protoplast (V/V_i), which is a function of the time (t) needed for the protoplast to equilibrate with the initial environmental solution of osmolality C_i after being quickly transferred to a final environmental solution with an osmolality of C_f; V_i is the initial volume of the protoplast; $a = Ci/Cf$; A is the initial surface area of the protoplast; and v_w is the molar volume of water. β is the fraction of the non-osmotic active volume of the whole protoplast volume at the initial state. The unknown parameters β and Pos are obtained by fitting V_r at a series of time points t.

Competing Interests

The authors declare no competing interests.

Author contributions:

X.Y. Xia conceived and designed the experiments. H.Y. Gao performed the experiments and analyzed the data. L.J. An provided technical assistance and helped with some experiments. X.Y. Xia and H.Y. Gao wrote the manuscript.

Acknowledgements

This research was financially supported by Guangdong Basic and Applied Basic Research Foundation (2019A1515111043), Youth Innovative Talents Project by Educational Department of Guangdong Province (2019KQNCX057), and Scientific Research Project of the Traditional Chinese Medicine Bureau of Guangdong Province (20202104).

571 **References**

572 Bakır Y, Eldem V, Zararsiz G, Unver T (2016). Global transcriptome analysis reveals
573 significant differences in gene expression patterns between the non-hyperhydric and
574 hyperhydric leaves of *Prunus persica*. *Plant Genome* 9:

575 Bräutigam K, Vining KJ, Lafon-Placette C, Fossdal CG, Mirouze M, Marcos JG, Fluch S,
576 Fraga MF, Guevara MÁ, Abarca D (2013). Epigenetic regulation of adaptive
577 responses of forest tree species to the environment. *Ecology & Evolution* 3: 399-415

578 Cedar H, Bergman Y (2012). Programming of DNA methylation patterns. *Annual Review*
579 *of Biochemistry* 81: 97-117

580 Chen X, Zhou DX (2013). Rice epigenomics and epigenetics: challenges and
581 opportunities. *Current Opinion in Plant Biology* 16: 164-169

582 Cokus SJ, Feng S, Zhang X, Chen Z, Merriman B, Haudenschild CD, Pradhan S, Nelson
583 SF, Pellegrini M, Jacobsen SE (2008). Shotgun bisulfite sequencing of the
584 *Arabidopsis* genome reveals DNA methylation patterning. *Nature* 452: 215-219

585 Dries NVD, Giannì S, Czerednik A, Krens FA, Klerk GJMD (2013). Flooding of the
586 apoplast is a key factor in the development of hyperhydricity. *Journal of*
587 *Experimental Botany* 64: 5221-5230

588 Fal MA, Majada JP, González A, Tamés RS (1999). Differences between *Dianthus*
589 *caryophyllus* L. cultivar in *in vitro* growth and morphogenesis are related to their
590 ethylene production. *Plant Growth Regulation* 27: 131-136

591 Feng H, Conneely KN, Wu H (2014). A Bayesian hierarchical model to detect
592 differentially methylated loci from single nucleotide resolution sequencing data.
593 *Nucleic Acids Research* 42: e69
594 Franck T, Kevers C, Gaspar T, Dommes J, Deby C, Greimers R, Serteyn D, Deby-Dupont
595 G (2004). Hyperhydricity of *Prunus avium* shoots cultured on gelrite: a controlled
596 stress response. *Plant Physiology & Biochemistry* 42: 519-527
597 Furner IJ, Matzke M (2011). Methylation and demethylation of the *Arabidopsis* genome.
598 *Current Opinion in Plant Biology* 14: 137-141
599 Gao H, Li J, Ji H, An L, Xia X (2017a). Hyperhydricity-induced ultrastructural and
600 physiological changes in blueberry (*Vaccinium* spp.). *Plant Cell Tissue & Organ*
601 *Culture* 133: 1-12
602 Gao H, Xia X, An L, Xin X, Liang Y (2017b). Reversion of hyperhydricity in pink
603 (*Dianthus chinensis* L.) plantlets by $AgNO_3$ and its associated mechanism during *in*
604 *vitro* culture. *Plant Science* 254: 1-11
605 Gao H, Xu P, Li J, Ji H, An L, Xia X (2017c). $AgNO_3$ prevents the occurrence of
606 hyperhydricity in *Dianthus chinensis* L. by enhancing water loss and antioxidant
607 capacity. *In Vitro Cellular & Developmental Biology - Plant* 53: 561-570
608 Gazzani S, Gendall AR, Lister C, Dean C (2003). Analysis of the molecular basis of
609 flowering time variation in *Arabidopsis* accessions. *Plant Physiology* 132:
610 1107-1114
611 Gehring M, Henikoff S (2009). Extensive demethylation of repetitive elements during

612 seed development underlies gene imprinting. *Science* 324: 1447-1451
613 Hassannejad S, Bernard F, Mirzajani F, Gholami M (2012). SA improvement of
614 hyperhydricity reversion in *Thymus daenensis* shoots culture may be associated with
615 polyamines changes. *Plant Physiology & Biochemistry* 51: 40-46
616 He XJ, Chen T, Zhu JK (2011). Regulation and function of DNA methylation in plants
617 and animals. *Cell Research* 21: 442
618 Hirayama T, Shinozaki K (2010). Research on plant abiotic stress responses in the
619 post-genome era: past, present and future. *Plant Journal* 61: 1041-1052
620 Hsieh TF, Ibarra CA, Silva P, Zemach A, Eshedwilliams L, Fischer RL, Zilberman D
621 (2009). Genome-wide demethylation of *Arabidopsis* endosperm. *Science* 324:
622 1451-1454
623 Ivanova M, Staden JV (2010). Natural ventilation effectively reduces hyperhydricity in
624 shoot cultures of *Aloe polyphylla* Schönland ex Pillans. *Plant Growth Regulation* 60:
625 143-150
626 Ivanova M, Staden JV (2011). Influence of gelling agent and cytokinins on the control of
627 hyperhydricity in Aloe polyphylla. *Plant Cell Tissue & Organ Culture* 104: 13-21
628 Jin L, Mao K, Li J, Huang W, Che T, Fu Y, Tang Q, Liu P, Song Y, Liu R (2018).
629 Genome-wide profiling of gene expression and DNA methylation provides insight
630 into low-altitude acclimation in Tibetan pigs. *Gene* 642: 522
631 Kevers C, Franck T, Strasser RJ, Gaspar T (2004). Hyperhydricity of micropropagated
632 shoots: a typically stress-induced change of physiological state. *Plant Cell Tissue &*

633 *Organ Culture* 77: 181-191
634 Krueger F, Andrews SR (2011). Bismark: a flexible aligner and methylation caller for
635 Bisulfite-Seq applications. *Bioinformatics* 27: 1571-1572
636 Lai CC, Lin HM, Nalawade SM, Fang W, Tsay HS (2005). Hyperhydricity in shoot
637 cultures of *Scrophularia yoshimurae* can be effectively reduced by ventilation of
638 culture vessels. *Journal of Plant Physiology* 162: 355-361
639 Lentini Z, Mussell H, Mutschler MA, Earle ED (1988). Ethylene generation and reversal
640 of ethylene effects during development in vitro of rapid-cycling Brassica campestris
641 L. *Plant Science* 54: 75-81
642 Li Q, Eichten SR, Hermanson PJ, Zaunbrecher VM, Song J, Wendt J, Rosenbaum H,
643 Madzima TF, Sloan AE, Huang J (2014). Genetic perturbation of the maize
644 methylome. *Plant Cell* 26: 4602
645 Mensuali-Sodi A, Panizza M, Serra G, Tognoni F (1993). Involvement of activated
646 charcoal in the modulation of abiotic and biotic ethylene levels in tissue cultures.
647 *Scientia Horticulturae* 54: 49-57
648 Mirouze M, Paszkowski J (2011). Epigenetic contribution to stress adaptation in plants.
649 *Current Opinion in Plant Biology* 14: 267-274
650 Muneer S, Park YG, Jeong BR (2017). Red and blue light emitting diodes (LEDs)
651 participate in mitigation of hyperhydricity in *in vitro*-grown carnation genotypes
652 (*Dianthus caryophyllus*). *Journal of Plant Growth Regulation*: 1-10
653 Muneer S, Soundararajan P, Jeong BR (2016). Proteomic and antioxidant analysis

654 elucidates the underlying mechanism of tolerance to hyperhydricity stress in *in vitro*
655 shoot cultures of *Dianthus Caryophyllus*. *Journal of Plant Growth Regulation* 35:
656 667-679
657 Ongabdullah M, Ordway JM, Jiang N, Ooi SE, Kok SY, Sarpan N, Azimi N, Hashim AT,
658 Ishak Z, Rosli SK (2015). Loss of Karma transposon methylation underlies
659 the mantled somaclonal variant of oil palm. *Nature* 525: 533-537
660 Park Y, Wu H (2016). Differential methylation analysis for BS-seq data under general
661 experimental design. *Bioinformatics* 32: 1-10
662 Qing D, Yang Z, Li M, Wong WS, Guo G, Liu S, Guo H (2016). Quantitative and
663 functional phosphoproteomic analysis reveals that ethylene regulates water transport
664 via the C-terminal phosphorylation of aquaporin PIP2;1 in *Arabidopsis*. *Molecular*
665 *plant* 9: 158-174
666 Saher S, Piqueras A, Hellin EE (2010). Hyperhydricity in micropropagated carnation
667 shoots: the role of oxidative stress. *Physiologia Plantarum* 120: 152-161
668 Sahu PP, Pandey G, Sharma N, Puranik S, Muthamilarasan M, Prasad M (2013).
669 Epigenetic mechanisms of plant stress responses and adaptation. *Plant Cell Reports*
670 32: 1151-1159
671 Saze H, Scheid OM, Paszkowski J (2003). Maintenance of CpG methylation is essential
672 for epigenetic inheritance during plant gametogenesis. *Nature Genetics* 34: 65-69
673 Sivanesan I, Saini RK, Kim DH (2016). Bioactive compounds in hyperhydric and normal
674 micropropagated shoots of *Aronia melanocarpa* (Michx.) Elliott. *Industrial Crops &*

675 *Products* 83: 31-38
676 Song, QingXin, Lu, Xiang, Li, QingTian, Chen, Hui, Hu, XingYu (2013). Genome-wide
677 analysis of DNA methylation in soybean. 6: 1961-1974
678 Soundararajan P, Manivannan A, Cho YS, Jeong BR (2017). Exogenous Supplementation
679 of Silicon improved the recovery of hyperhydric shoots in *Dianthus caryophyllus* L.
680 by stabilizing the physiology and protein expression. *Frontiers in Plant Science* 8:
681 Tabart J, Franck T, Kevers C, Dommes J (2015). Effect of polyamines and polyamine
682 precursors on hyperhydricity in micropropagated apple shoots. *Plant Cell Tissue &*
683 *Organ Culture* 120: 11-18
684 Tian J, Jiang F, Wu Z (2015). The apoplastic oxidative burst as a key factor of
685 hyperhydricity in garlic plantlet in vitro. *Plant Cell Tissue & Organ Culture* 120:
686 571-584
687 Wu H, Xu T, Feng H, Chen L, Li B, Yao B, Qin Z, Jin P, Conneely, N. K (2015).
688 Detection of differentially methylated regions from whole-genome bisulfite
689 sequencing data without replicates. *Nucleic Acids Research* 43: e141-e141
690 Wu XN, Sanchez RC, Pertl-Obermeyer H, Obermeyer G, Schulze WX (2013).
691 Sucrose-induced receptor kinase SIRK1 regulates a plasma membrane aquaporin in
692 *Arabidopsis*. *Molecular & Cellular Proteomics* 12: 2856-2873
693 Xu J, Zhou S, Gong X, Song Y, Van NS, Ma F, Guan Q (2018). Single-base methylome
694 analysis reveals dynamic epigenomic differences associated with water deficit in
695 apple. *Plant Biotechnology Journal* 16: 672-687

696 Young MD, Wakefield MJ, Smyth GK, Oshlack A (2010). Gene ontology analysis for
697 RNA-seq: accounting for selection bias. *Genome Biology* 11: R14-R14
698 Zemach A, Kim MY, Silva P, Rodrigues JA, Dotson B, Brooks MD, Zilberman D (2010).
699 Local DNA hypomethylation activates genes in rice endosperm. *Proceedings of the*
700 *National Academy of Sciences of the United States of America* 107: 18729-18734

701

Supplemental Data

Supplemental Figure S1. ML of different genic regions in the context of CG, CHG and CHH. The X-axis represents different gene elements, and the Y-axis represents the ML.

Supplemental Figure S2. Circular plots of DMRs. Track order: hyper-DMR; density of TEs; gene density of each chromosome; hypo-DMR. The higher the density of the dot, the more significant the difference in DMR.

Supplemental Figure S3. The most enriched GO terms of genes with CHH DMRs (C) and genes whose promoters have DMRs (D) in normal and hyperhydric seedlings. (* represents statistical significance at the $P \leqslant 0.05$ level).

Supplemental Figure S4. Differentially expressed genes (DEGs) between HH and normal. Each dot represents one gene. The red dots represent up-regulated genes and the green dots represent down-regulated genes. The blue dots represent genes without differential expression. The X-axis is the $\log_2$ value of fold change and the Y-axis is the $\log_{10}$ value of the *P*-value.

Supplemental Figure S5. Scatter and box plots of correlated DMR methylation and RNA expression affecting genes involved in HH. Scatter and box plots of correlated DMRs and RNA expression in CG (A), CHG (B) and CHH (C) contexts. Top left picture: box diagram of DMR-related gene expression levels. Top right picture: Comparison of the ML and expression level of DMR-related genes; the horizontal coordinates represent the gene ML, and the ordinate represents the gene expression level. Bottom left legend: promoter/gene body hyper/hypo represents the ML of the promoter/gene body region in

the hyper/hypo-DMR, rho represents the correlation coefficient between the gene ML and expression level in the scatter plot, and rho.p-val represents the correlation P-value. Bottom right picture: Comparison of the ML of the DMR-related genes in the form of a box diagram. The black colour represents hyperhydric seedlings, and the blue colour represents normal seedlings.

Supplemental Figure S6. Gene ontology (GO) analysis of ethylene-related CHH hypo DMR (A) and DMR promoter (B) genes between HH and normal.

Supplemental Figure S7. Development of HH in *Arabidopsis* mutants.

Supplemental Figure S8. Expression of genes associated with ethylene biosynthesis and signal transduction. *SAM*, *ACS1* and *ACO* are genes related to ethylene biosynthesis; *ETR1* and *ETR2* are ethylene receptor genes; and *ERF12* and *ERF113* are ethylene response genes. The expression levels of genes in whole seedlings were quantified by qRT-PCR and normalized against the expression level of *actin*. The data are the means ± SEs, and the values are presented as fold changes in expression (hyperhydric seedlings cultured in Gelrite or Gelrite supplemented with $AgNO_3$ versus normal seedlings in normal culture media). Statistical significance was calculated by Student's t-test, '*' indicates a significant difference at the $P < 0.05$ level.

Supplemental Table S1. Data description of the BS-Seq reads for the three *Arabidopsis* samples with three replicates.

Supplemental Table S2. Percentage of methylation levels of normal and HH seedlings.

Supplemental Table S3. Ethylene-related CHH hypo genes between HH and normal

744 seedlings.

745 **Supplemental Table S4.** Primers used for the bisulphite sequencing analysis.

746 **Supplemental Table S5.** Primers used for the qRT-PCR analysis.

Figure Legends

Fig. 1. Phenotypic and DNA methylome differences between hyperhydric and normal seedlings of *Arabidopsis thaliana*. (A) Development of HH in *Arabidopsis* seedlings. Images were taken after 14 days of culture on 0.7% agar (Normal) or 0.2% Gelrite (HH). (B) Relative proportions of three sequence contexts (CG, CHG and CHH) for all mCs. (C) Analysis of DMRs in hyperhydric seedlings compared with normal seedlings. Numbers of DMR-overlapping promoter, TSS, 5'UTR, exon, intron, 3'UTR, TES, repeat and other regions. (D) Venn diagram of genes with DMRs and genes whose promoters have DMRs in normal and hyperhydric seedlings.

Fig. 2. Analysis of DEGs in hyperhydric versus normal seedlings. (A) Assignments of DEGs in hyperhydric and normal seedlings, as shown in MapMan bins. The red and blue squares indicate up- and downregulated genes, respectively. Venn diagram of DEGs with DMRs (B) and DEGs whose promoters have DMRs (C) in hyperhydric versus normal seedlings.

Fig. 3. Effects of $AgNO_3$ on the morphology and water content of *Arabidopsis* hyperhydric seedlings. (A) Effects of $AgNO_3$ on the morphology of seedlings cultured on Gelrite. (B) Changes in the water content of the different groups of seedlings after 14 days of culture. (C) Changes in endogenous ethylene accumulation of the different groups of seedlings in their respective media during the 14 days growth period. The data are the means ± SEs of three leaf samples randomly taken from nine seedlings. The statistical significance was calculated by Student's t-test, '*' indicates a significant difference at the

770 P < 0.05 level. (D) Analysis of *ACS1* and *ETR1* promoter DNA methylation and
771 expression. Analysis of the cytosine methylation of a 350 bp segment spanning the *ACS1*
772 and *ETR1* promoter. Twenty clones per DNA sample were analyszed. The filled circles
773 represent methylated cytosines, and the empty circles represent unmethylated contexts.
774
775 **Fig. 4.** Phosphorylation of PIP2;1 and protoplast swelling assay results. (A) Relative
776 phosphorylation levels of endogenous PIP2;1 protein in normal seedlings, hyperhydric
777 seedlings and seedlings grown in media supplemented with $AgNO_3$, as detected by
778 anti-pS283 polyclonal antibodies. (B) *V/Vi* of protoplasts during swelling experiments.
779 The means ± SEs of volume change at each time point were obtained from the analysis of
780 20 protoplasts generated from five independent protoplast preparations. *V/Vi* is equal to
781 the swelling volume divided by the initial volume. (C) Average *Pos* of protoplasts in
782 different groups of seedlings. The data are the means ± SEs (n = 20). Statistical
783 significance was calculated by Student's t-test, '*' indicates a significant difference at the
784 P < 0.05 level.
785
786 **Fig. 5.** Influence of HH on stomatal aperture and water loss in *Arabidopsis* seedlings. (A)
787 Confocal micrographs of H_2DCFDA-stained guard cells and quantification of subcellular
788 DCF fluorescence of normal seedlings, hyperhydric seedlings and seedlings grown in
789 media supplemented with $AgNO_3$. The data are the means ± SEs of 90 stomata from three
790 independent replicates. (B) Microscopic images of the abaxial epidermis of leaves of
791 normal seedlings, hyperhydric seedlings and seedlings grown in media supplemented
792 with $AgNO_3$. Scale bar = 50 μm. (C) Changes in stomatal aperture of the different groups

of seedlings. (D) Changes in water loss of the different groups of seedlings. The data are the mean ± SEs from 10 leaf samples randomly taken from ten selected seedlings. Statistical significance was calculated by Student's t-test, '*' indicates a significant difference at the $P < 0.05$ level.

Fig. 6. Proposed mechanism for the ethylene-induced development of HH in *Arabidopsis*.

Supplemental Materials

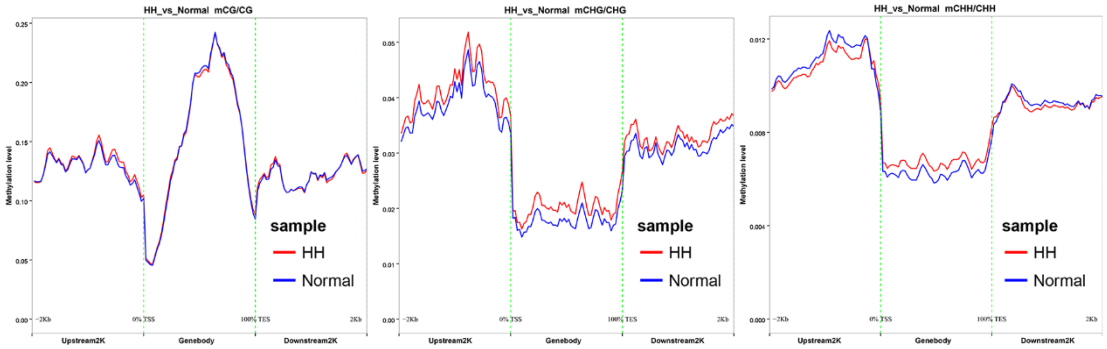

Supplemental Figure S1. ML of different genic regions in the context of CG, CHG and CHH. The X-axis represents different gene elements, and the Y-axis represents the ML.

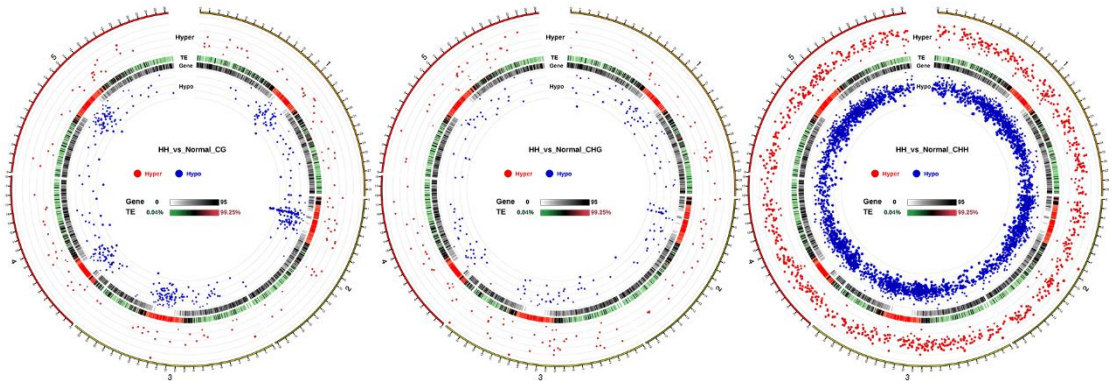

Supplemental Figure S2. Circular plots of DMRs. Track order: hyper-DMR; density of TEs; gene density of each chromosome; hypo-DMR. The higher the density of the dot, the more significant the difference in DMR.

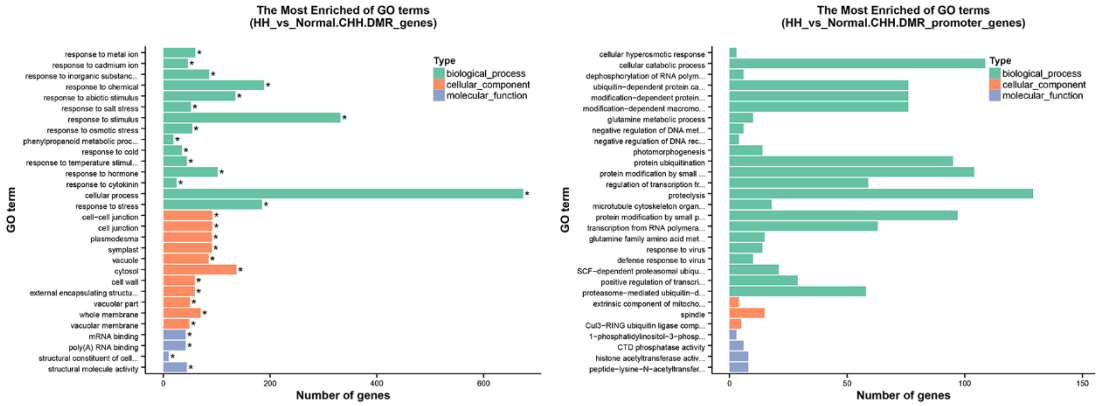

10

11 **Supplemental Figure S3.** The most enriched GO terms of genes with CHH DMRs (C)

12 and genes whose promoters have DMRs (D) in normal and hyperhydric seedlings. (*

13 represents statistical significance at the $P \leq 0.05$ level).

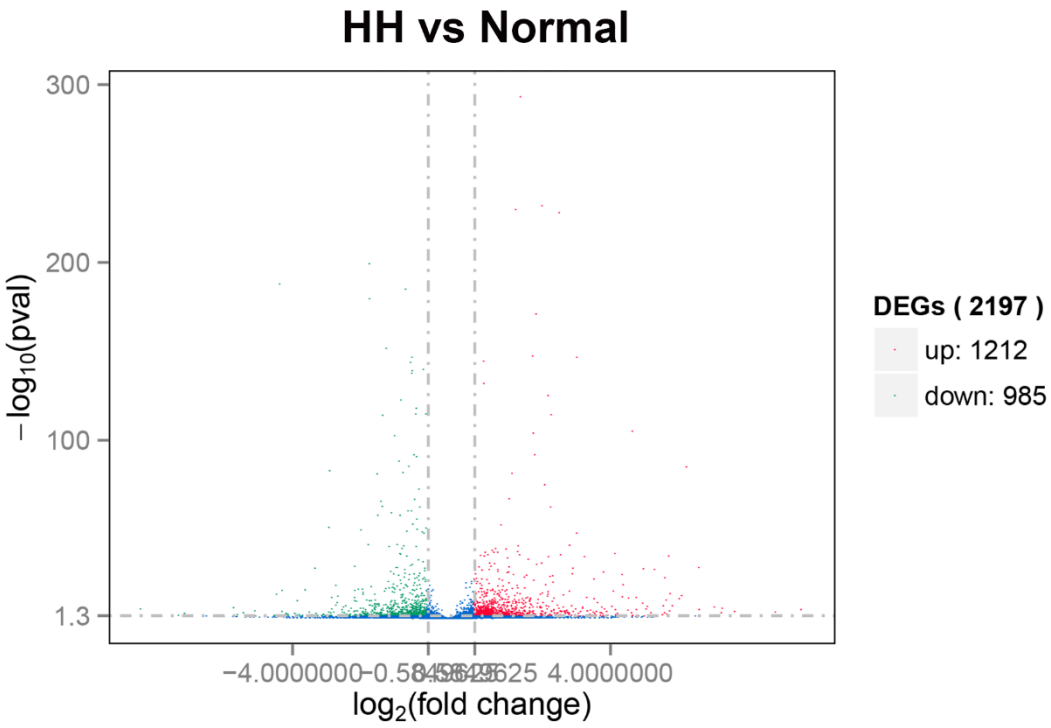

14

15 **Supplemental Figure S4.** Differentially expressed genes (DEGs) between HH and

16 normal. Each dot represents one gene. The red dots represent up-regulated genes and

17 the green dots represent down-regulated genes. The blue dots represent genes without

differential expression. The X-axis is the $\log_2$ value of fold change and the Y-axis is the $\log_{10}$ value of the P-value.

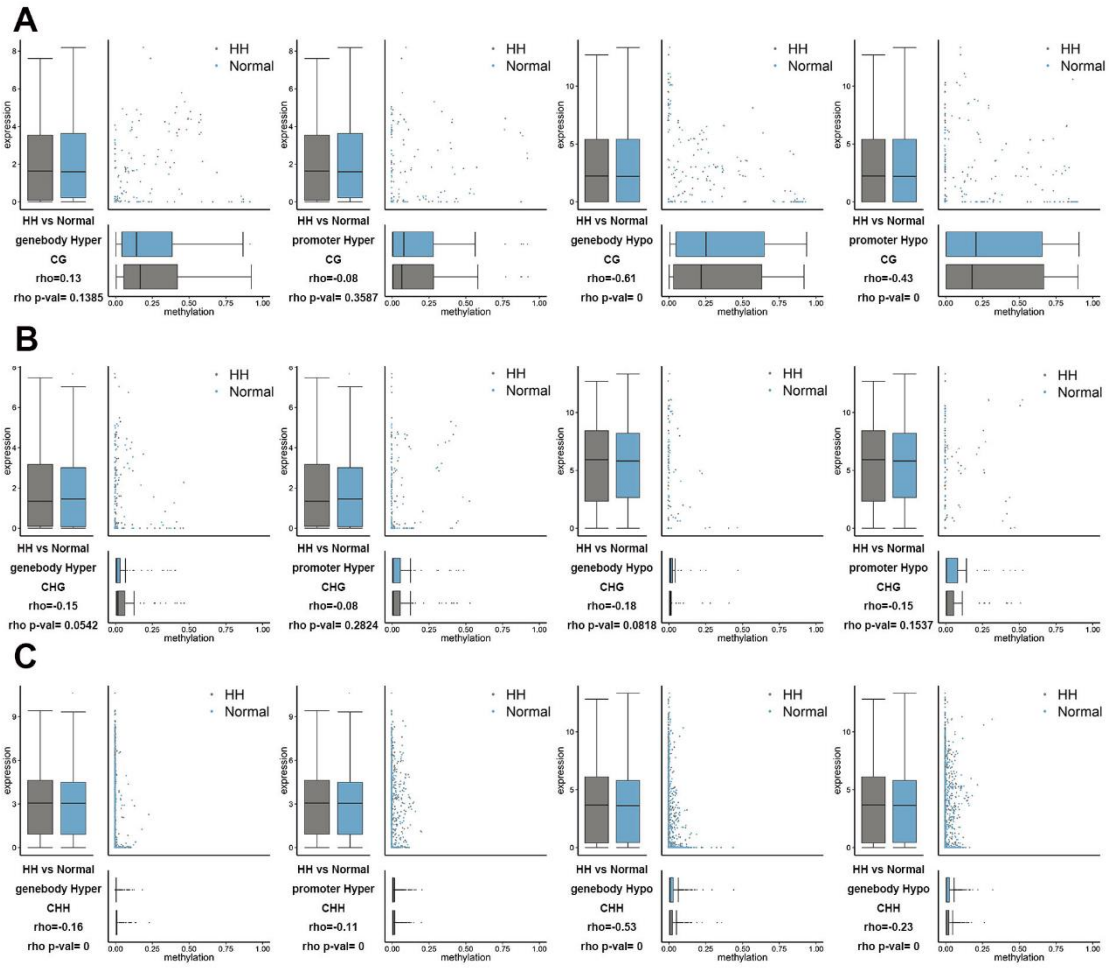

Supplemental Figure S5. Scatter and box plots of correlated DMR methylation and RNA expression affecting genes involved in HH. Scatter and box plots of correlated DMRs and RNA expression in CG (A), CHG (B) and CHH (C) contexts. Top left picture: box diagram of DMR-related gene expression levels. Top right picture: Comparison of the ML and expression level of DMR-related genes; the horizontal coordinates represent the gene ML, and the ordinate represents the gene expression

level. Bottom left legend: promoter/gene body hyper/hypo represents the ML of the promoter/gene body region in the hyper/hypo-DMR, rho represents the correlation coefficient between the gene ML and expression level in the scatter plot, and rho.p-val represents the correlation P-value. Bottom right picture: Comparison of the ML of the DMR-related genes in the form of a box diagram. The black colour represents hyperhydric seedlings, and the blue colour represents normal seedlings.

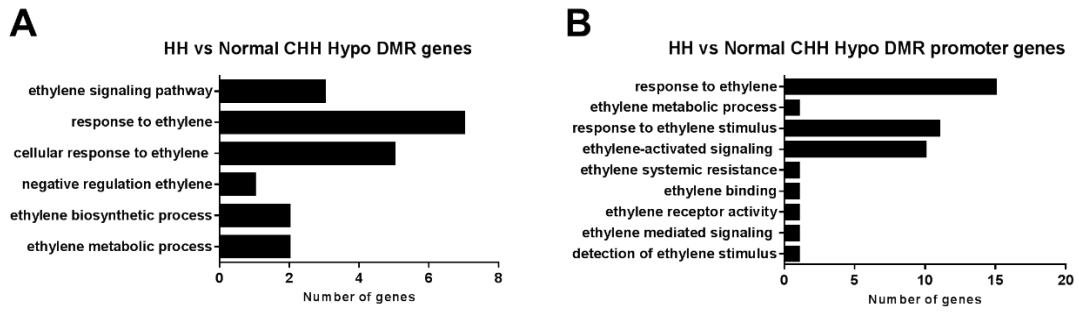

Supplemental Figure S6. Gene ontology (GO) analysis of ethylene-related CHH hypo DMR (A) and DMR promoter (B) genes between HH and normal.

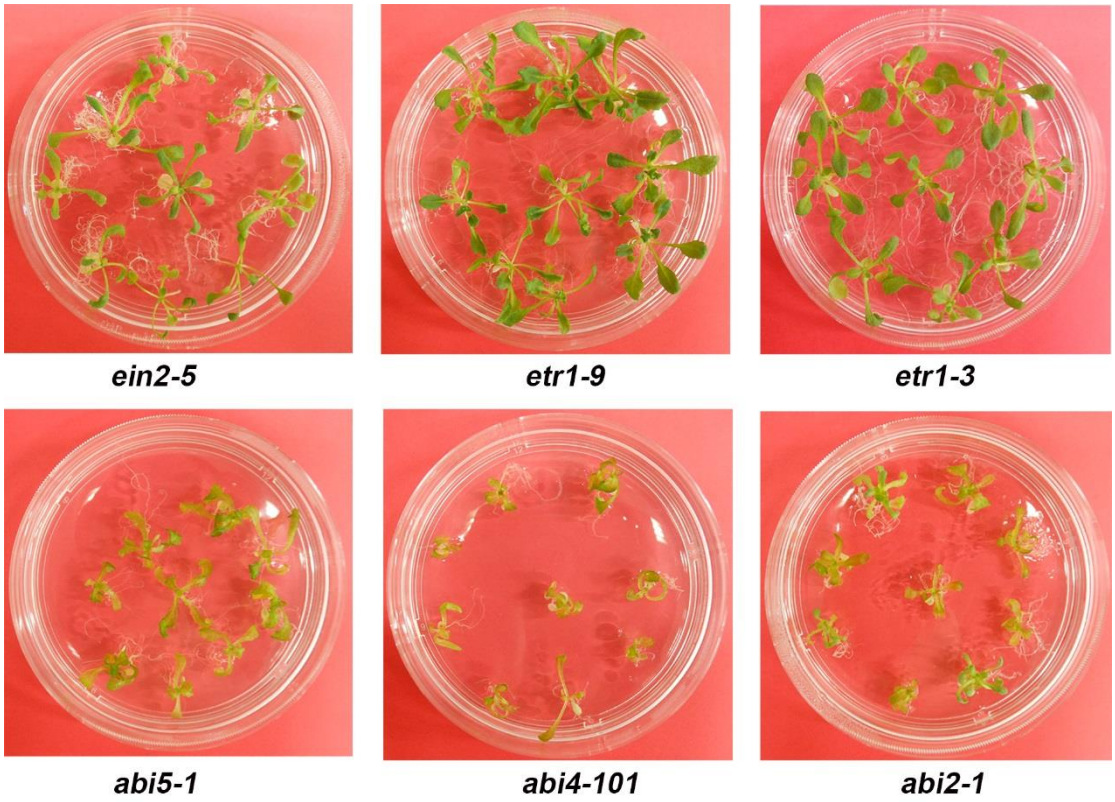

Supplemental Figure S7. Development of HH in *Arabidopsis* mutants.

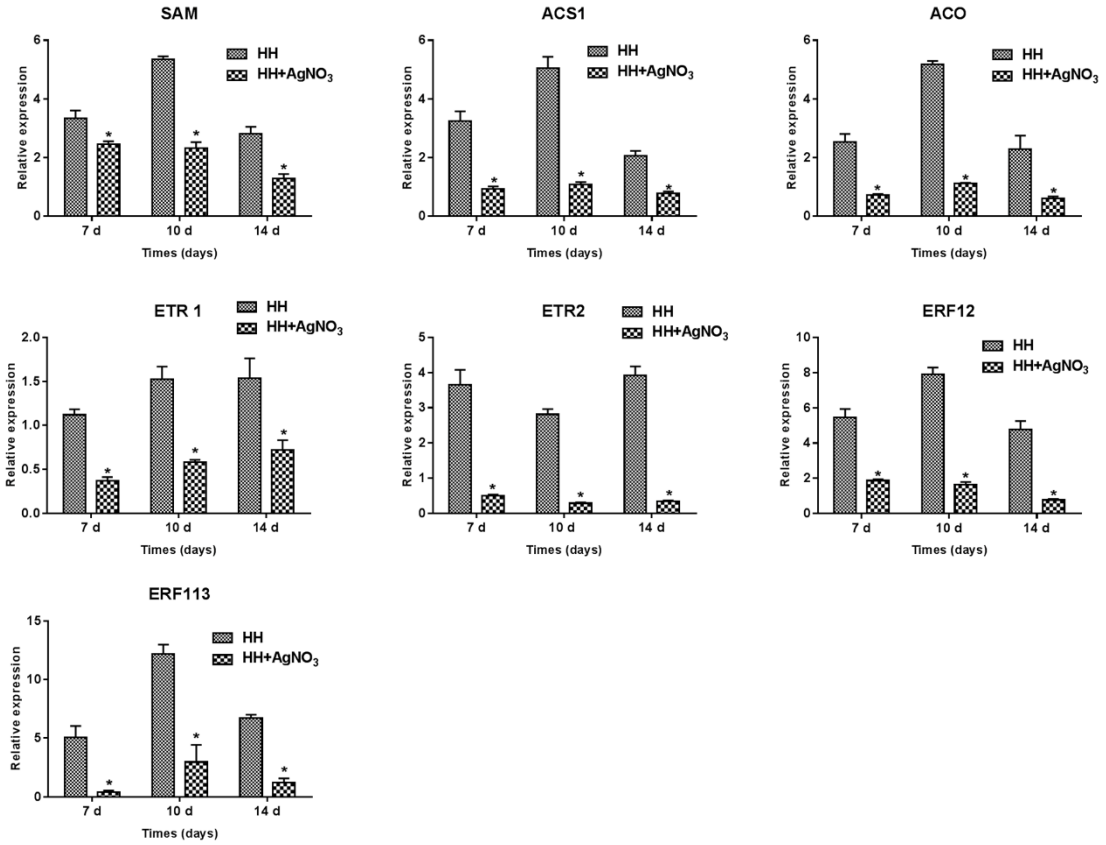

Supplemental Figure S8. Expression of genes associated with ethylene biosynthesis and signal transduction. *SAM*, *ACS1* and *ACO* are genes related to ethylene biosynthesis; *ETR1* and *ETR2* are ethylene receptor genes; and *ERF12* and *ERF113* are ethylene response genes. The expression levels of genes in whole seedlings were quantified by qRT-PCR and normalized against the expression level of *actin*. The data are the means ± SEs, and the values are presented as fold changes in expression (hyperhydric seedlings cultured in Gelrite or Gelrite supplemented with $AgNO_3$ versus normal seedlings in normal culture media). Statistical significance was calculated by Student's t-test, '*' indicates a significant difference at the $P < 0.05$ level.

Supplemental Table S1. Data description of BS-Seq reads for the three *Arabidopsis* samples with three replicates.

Sample	Raw Resds/ Raw bases(G)	Clean reads/ Clean_bases(G)	BS conversion rate (%)	Mapping rate (%)	Duplication rate (%)
Normal 1	32486404/8.12	32417623/7.91	99.635	77.89	2.57
Normal 2	34917325/8.73	34157825/8.29	99.686	75.23	3.43
Normal 3	29215929/7.30	29159617/7.11	99.655	79.94	3.48
HH 1	28981333/7.25	27905322/6.69	99.462	66.67	5.07
HH 2	36679885/9.17	35438899/8.57	99.677	74.77	3.38
HH 3	36460895/9.12	35266713/8.54	99.650	72.30	3.60

Supplemental Table S2. Percentage of methylation levels of normal and HH.

Sample	C (Mb)	mC %	CG (Mb)	mCG %	CHG (Mb)	mCHG %	CHH (Mb)	mCHH %
Normal 1	902.5	10.8%	128.0	30.35%	131.9	17.24%	642.6	6.05%
Normal 2	869.3	10.79%	131.5	29.96%	132.6	17.66%	605.2	6.02%
Normal 3	762.3	10.7%	111.3	27.99%	111.6	16.78%	539.3	6.42%
HH 1	581.7	9.06%	94.1	24.41%	90.0	15.42%	397.7	5.08%
HH 2	909.1	10.13%	133.4	30.49%	134.9	17.57%	640.7	5.04%
HH3	871.2	10.54%	130.5	29.93%	131.5	17.4%	609.1	5.73%

Supplemental Table S3. Ethylene-related CHH hypo genes between HH and normal.

Gene_id	Gene name	Methylation difference	Region	Description
HH vs Normal CHH Hypo DMR genes				
AT1G05010	ACO4	-0.0588	exon	ethylene-forming enzyme
AT1G02500	SAM1	-0.02	exon	S-adenosylmethionine synthetase
AT5G03730	CTR1	-0.035	exon	Protein kinase superfamily protein
AT1G05850	CTL1	-0.033	3'UTR, exon	Chitinase family protein
AT5G04950	NAS1	-0.029	exon	nicotianamine synthase 1
AT3G15730	PLDALPHA1	-0.025	Exon, 3'UTR	phospholipase D alpha 1
AT4G19690	IRT1	-0.021	exon	iron-regulated transporter 1
AT2G05520	GRP3	-0.059	Exon, 3'UTR	Glycine rich protein
AT1G49950	TRB1	-0.08	Exon, 3'UTR	telomere repeat binding factor 1
HH vs Normal CHH Hypo DMR promoter genes				
AT1G66340	ETR1	-0.074	promoter	Signal transduction response regulator
AT3G61510	ACS1	-0.03	promoter	1-aminocyclopropane-1-carboxylate synthase 1
AT1G56160	ATMYB72	-0.034	promoter	Myb domain protein 72
AT1G22190	RAP2-13	-0.102	promoter	AP2/ERF domain
AT2G40220	ABI4	-0.086	promoter	AP2/ERF domain;

AT1G06160	ERF094	-0.089	promoter	ethylene response factor
AT3G15010	UBA2C	-0.024	promoter	RNA-binding (RRM/RBD/RNP motifs) family protein
AT1G46768	RAP2-1	-0.087	promoter	AP2/ERF domain
AT5G42190	SKP1B	-0.058	promoter	E3 ubiquitin ligase SCF complex subunit SKP1/ASK1 family protein
AT5G44210	ERF9	-0.054	promoter	ethylene response factor
AT2G21150	XCT	-0.049	promoter	XAP5 family protein
AT1G28160	ERF087	-0.074	promoter	ethylene response factor
AT5G02320	MYB3R5	-0.073	promoter	myb domain protein 3r-5
AT5G24520	TTG1	-0.043	promoter	Transducin/WD40 repeat-like superfamily protein
AT4G05100	AtMYB74	-0.092	promoter	myb domain protein 74
AT1G05690	BT3	-0.072	promoter	BTB and TAZ domain protein 3

Supplemental Table S4. Primer sequences used for bisulphite sequencing analysis.

Gene name	Gene ID	Forward primer (5'→3')	Reverse primer (5'→3')
ACS1	AT3G61510	TAGGGTATTTATYGAGGGATTTG	AATATTAACACRTAAAACAACCCAC
ETR1	AT1G66340	TTGGAAATTTATAAAATTTAATATAGTAAA	CTATAAAAAATAATACAAATCRATAAATT

Supplemental Table S5. Primer sequences used for real-time PCR analysis.

Gene name	Gene ID	Forward primer (5'→3')	Reverse primer (5'→3')
SAM	AT3G17390	GGATCTGAAGAGAGGAGGTAA	GACTTGAGTGGCTTGACTAC
ACS1	AT3G61510	TGAGTGACAAACATGGAGAAG	GGCGAGACCCATTTGAATAA
ACO	AT2G19590	CTTATGAGAGGGCTGAGAGA	GTTCTTGGATGGCGGTATAG
ETR1	AT1G66340	GCTAGACGAGAAGCAGAAAC	GAGTAAGGAAGAGAGTGCAATAA
ETR2	AT3G23150	CTGGATTCGATTGCCTTACC	CCTCATGGCCACTTCATAAC
ERF12	AT1G21910	CAAAGGAGTGAGGATGAGAAG	GCTTCAGCTGTTGAGTAAGA
ERF113	AT5G13330	GTAAATGGGCGGCAGAAA	AGCTCGGTCATAGGCTAAA
ACTIN	AT3G18780	GGTAACATTGTGCTCAGTGGTGG	AACGACCTTAATCTTCATGCTGC